Multipath Triangulation: Decimeter-level WiFi Localization and Orientation with a Single Unaided Receiver

Elahe Soltanaghaei
University of Virginia
Charlottesville, VA,USA
es3ce@virginia.edu

Avinash Kalyanaraman
University of Virginia
Charlottesville, VA,USA
ak3ka@virginia.edu

Kamin Whitehouse
University of Virginia
Charlottesville, VA,USA
whitehouse@virginia.edu

ABSTRACT

Decimeter-level localization has become a reality, in part due to the ability to eliminate the effects of multipath interference. In this paper, we demonstrate the ability to use multipath reflections to enhance localization rather than throwing them away. We present *Multipath Triangulation*, a new localization technique that uses multipath reflections to localize a target device with a single receiver that does not require any form of coordination with any other devices. In this paper, we leverage *multipath triangulation* to build the first decimeter-level WiFi localization system, called *MonoLoco*, that requires only a single access point (AP) and a single channel, and does not impose any overhead, data sharing, or coordination protocols beyond standard WiFi communication. As a bonus, it also determines the orientation of the target relative to the AP. We implemented MonoLoco using Intel 5300 commodity WiFi cards and deploy it in four environments with different multipath propagation. Results indicate median localization error of $0.5m$ and median orientation error of 6.6 degrees, which are comparable to the best performing prior systems, all of which require multiple APs and/or multiple frequency channels. High accuracy can be achieved with only a handful of packets.

KEYWORDS

multipath triangulation, localization, multipath propagation, WiFi, Channel State Information, CSI

ACM Reference Format:
Elahe Soltanaghaei, Avinash Kalyanaraman, and Kamin Whitehouse. 2018. Multipath Triangulation: Decimeter-level WiFi Localization and Orientation with a Single Unaided Receiver. In *MobiSys '18: The 16th Annual International Conference on Mobile Systems, Applications, and Services, June 10–15, 2018, Munich, Germany*. ACM, New York, NY, USA, 13 pages. https://doi.org/10.1145/3210240.3210347

1 INTRODUCTION

In recent years, several new developments have enabled RF localization with tens of centimeters error – a promising and important step towards the vision of accurate and ubiquitous indoor device localization. A common thread that runs through this new generation of techniques is the ability to eliminate the effects of multipath interference by directly measuring geometric features of the line of sight (LoS) signal, such as angle of arrival (AoA) or time of flight (ToF). However, due to fundamental limits in clock synchronization or range resolution, current methods require some form of explicit coordination between nodes. For example, AoA-based methods require coordination across multiple access points (APs) to perform triangulation; and ToF-based methods require establishing two-way communication as well as channel switching between the transmitter and receiver to overcome the challenge of clock synchronization and bandwidth limitation. Coordination between nodes can take many forms but cannot be achieved without introducing complexity, communication overhead, pre-deployed infrastructure, and/or the practical challenges of protocol rollout and adoption.

In this paper, we present a different approach to WiFi localization: instead of eliminating the effects of multipath reflections, we use them to help localize the transmitter. Every multipath reflection is considered to be an independent measurement of the target location. We extract features of the multipath signals, including their angle of arrival (AoA), angle of departure (AoD), and relative time of flight (rToF), i.e. their ToF relative to that of the LoS path. These multipath features are combined with the AoA and AoD of the LoS path to form a *multipath triangle* between the target device, the receiver, and the reflector. The key insight behind our approach is that the geometry of this triangle is fully constrained; the AoA and AoD of the two paths define the shape and orientation of the triangle while the rToF uniquely defines its scale. As such, it can be used to triangulate the position of the transmitter relative to the receiver. In effect, this approach uses multipath reflections in the same way that conventional triangulation uses multiple APs. We call this approach *multipath triangulation*.

The main benefit of *multipath triangulation* is that it enables what we call *unaided device localization*: a single receiver can localize a transmitting target without coordinating with any other nodes. It avoids coordination with APs by using multipath reflections to triangulate the target location, and it avoids coordinating with the transmitter by measuring rToF instead of absolute ToF. Unlike ToF, rToF can be measured entirely at the receiver without coordinating with the transmitter because it relies on relative phase values across frequencies, thus not requiring clock synchronization [18]. In contrast, existing systems require the APs to share their locations with mobile nodes [5, 32, 34], to share measurements with each other [9, 18, 22, 47], or to perform coordinated actions with the target node for time synchronization [7, 24] or frequency hopping [40, 48, 49]. Each of these methods incurs some challenges of

MobiSys '18, June 10–15, 2018, Munich, Germany

ACM ISBN 978-1-4503-5720-3/18/06…$15.00
https://doi.org/10.1145/3210240.3210347

coordination in terms of complexity, overhead, infrastructure, or adoption.

We leverage this feature of *multipath triangulation* to design *MonoLoco*, the first unaided WiFi localization system with decimeter-level accuracy that requires only a single commodity WiFi receiver and a single channel. As a bonus, it also provides the orientation of the target with degree-level accuracy. MonoLoco uses only Channel State Information (CSI) from a 3-element antenna array to derive AoA, AoD, and ToF of each path. It defines a new model of the wireless channel based on subspace-based super-resolution methods [18, 29, 33] that combines transmitting antennas, receiving antennas and multiple frequency subcarriers into a single large-aperture sensing array. Then, it plugs the derived AoA, AoD, and ToF into a non-linear optimization problem to determine the location and orientation of the target. CSI is already collected by commercial WiFi chipsets without requiring a firmware upgrade, and multi-element arrays are commonly used on APs, laptops, drones, televisions, and many other devices. As such, MonoLoco is *fully-piggybacked* on top of WiFi communication; it does not impose any requirements beyond standard WiFi protocols, including hardware changes, protocol overhead, external clocks, external sensors (such as inertial sensors), or environmental profiling. Thus, MonoLoco can be used opportunistically whenever these nodes happen to communicate, with no additional overhead.

Furthermore, CSI is measured from the packet preamble and, as such, can be measured for eavesdropped packets even without 802.11 association, and even if the packets are encrypted. Thus, MonoLoco allows any WiFi device to localize any other nearby WiFi device even if neither of them is an AP. For example, a home automation system can localize controllers such as smart thermostats or smart plugs (with respect to its own coordinate system), even if neither the controllers nor the home's AP(s) support a localization protocol. In addition, MonoLoco provides orientation estimates with degree-level accuracy, which can enable new context-based applications. For example, when a person asks a smart speaker for a picture or recipe, it can automatically cast the image to a display with a position and orientation that is visible from a given location. Similarly, a robot can navigate to a WiFi power socket while using its estimated orientation to determine the side of the wall from which to approach it.

To evaluate this approach, we implement MonoLoco using Intel 5300 WiFi cards operating at 5GHz with 40 MHz of bandwidth. Each node was equipped with a 3-element linear antenna array with 2.7 cm spacing between antennas. We deployed MonoLoco in four environments with different multipath properties, including an anechoic chamber, a home, two office environments, and two public spaces. Our experiments show that MonoLoco achieves a median localization error of 0.5 m and a median orientation error of 6.6 degrees, which are comparable to the best existing systems that require multi-node coordination. Results also show that MonoLoco can approach this accuracy with as few as 7 packets. These results are promising and serve as a proof-of-concept for the *multipath triangulation* approach. We expect these results to improve when used with more advanced resolution algorithms such as Maximum Likelihood methods [46] and non-linear solvers, which are now becoming computable. In addition, Results are also expected to improve when using more number of antennas or larger bandwidth, all of which are possible with today's WiFi chips.

Contributions: The main contributions of this paper include:

- *Multipath triangulation:* the first localization technique that can be used by a single unaided receiver. This method is general and can be applied beyond WiFi.
- *3D multipath super-resolution:* a new model for the multipath channel that enables super-resolution methods to estimate AoA and AoD with 26-36% higher accuracy than existing models and provides the relative ToF between paths.
- *MonoLoco:* the first WiFi localization system that simultaneously provides decimeter-level localization and degree-level orientation by only using CSI measurements from a single channel in a single receiver.

2 BACKGROUND AND RELATED WORK

In general, wireless localization schemes either map measurements from wireless signals into geometric parameters such as distance or direction to localize the target with respect to one or multiple reference devices, or prelabel landmarks to directly localize the target in the space. In this paper, we focus on the first scenario where two devices are localized with respect to each other. The state-of-the-art device localization systems can be categorized into (1) distance-based (or ToF-based) methods which leverage trilateration or multilateration, and (2) angle-based methods which use triangulation. However, using either of these methods requires some form of explicit coordination between nodes that is explained next.

Time of Flight (ToF) measurement is a widely used technique for device localization, which relies on measurements of travel time of signals between the transmitter and receiver. However, accurate measurement of ToF requires a common clock and strict time synchronization between the transmitter and receiver. To overcome this challenge, traditional ToF-based systems either use multiple synchronized transmitters such as the GPS system [28], or use the "echoing" method [23, 27, 31, 45, 51] where the transmitter measures the round trip propagation time. A problem with round-trip ToF-based systems is the response delay at the receiver which highly depends on the receiver electronics and protocol overheads. A recent system called Chronos [40] addresses this problem by leveraging the channel frequency responses and combining these measurements from both transmission directions. In effect, it can accurately estimate ToF by removing the sampling frequency offset caused by lack of time synchronization between two nodes. However, it still suffers from the fundamental limitation of the round-trip techniques, which is the required two-way communication and overhead of message exchanging between any two nodes to localize each other. Cricket [32] is a localization system that overcomes the synchronization problem by using a combination of RF and ultrasonic signals, however, it requires dedicated hardware.

Time Difference of Arrival (TDoA) is another technique to overcome the synchronization problem. It uses relative time measurements between multiple pairs of APs or reference nodes with known locations, instead of absolute time measurements [20, 48–50]. Each difference of arrival time measurement produces a hyperbolic curve

	Underlying Method	Decimeter-Level Localization	Orientation	Single Access Point	Unaided (No Coordination)	Fully Piggybacked
ToneTrack [49]	Multilateration	✗	✗	✗	✗	✗
PinLoc [34]	Fingerprinting	✗	✗	✗	✗	✓
SpotFi [18]	Triangulation	✓	✗	✗	✗	✓
Chronos [40]	Trilateration	✓	✗	✓	✗	✗
MonoLoco	Multipath Triangulation	✓	✓	✓	✓	✓

Table 1: Compared to the state-of-the-art of WiFi localization systems, MonoLoco is the only single access-point solution that provides decimeter-level localization and orientation information and requires no coordination, time synchronization or external networking protocol with the target or with other APs.

in the location space, so the TDoA from at least three receivers is required to find the intersection and accordingly the location of the transmitter. Although this technique does not need any time synchronization between the transmitter and receiver, it requires strict time synchronization between the access points.

Another component of ToF (or TDoA)-based localization systems is to convert the time (or distance) measurements into locations using geometric algorithms such as *trilateration* or *multilateration*. These algorithms localize the target by finding the intersection of distance measurements from multiple anchors, which mandates a centralized localization infrastructure with multiple access points or reference nodes to coordinate the localization together. Chronos[40] addresses this issue by performing trilateration between time-synchronized antennas separated by 30cm, however, it still requires coordination between the transmitter and receiver to share their channel measurements for clock synchronization. SAIL [27] is another system that can localize a target with a single access point using round trip ToF measurements. However, it relies on external IMU sensors on the target as well as target movement to perform trilateration.

Besides the synchronization error, the other factors that affect ToF (and TDoA) estimation accuracy are the signal bandwidth and the sampling rate. Time resolution is inversely related to the radio bandwidth, and low sampling rate (in time) reduces the ToF resolution since the signal may arrive between the sampled intervals. Some proposals such as Chronos [40] and ToneTrack [49] emulate wideband communication by switching between multiple channels and stitching measurements from these channels together to obtain the ToF with high resolution. However, not only these techniques do not overcome the required coordination for time synchronization, they even introduce new coordination between the transmitter and receiver for channel switching. Some other proposals address the bandwidth limitation by using frequency domain super-resolution algorithms [41, 42] and joint estimation of multiple geometric parameters [39].

Angle-based method or triangulation is another group of localization systems that either use beamforming (with directional antenna) to estimate the direction with maximum signal strength, or leverage relative phase measurements in an antenna array to estimate the angle of the LoS path. Although angle-based techniques do not suffer from time synchronization or bandwidth problem, they still require measurements from several (four to six) anchors simultaneously to perform triangulation [9, 18, 19, 22, 47], thus requiring information sharing and coordination of several nodes for accurate localization. In addition, very large antenna arrays (6-8 elements) are usually required [47] to improve the resolution.

Multipath triangulation builds on the state-of-the-art methods and combines the best features of angle-based and ToF-based methods. It avoids coordination between multiple APs by using angular features of multipath reflections such as Angle of Arrival (AoA) and Angle of Departure (AoD), and combining them with those of LoS path. In addition, it overcomes time synchronization problem by leveraging the difference in ToF of two paths instead of the absolute ToF to constrain the localization algorithm. Therefore, it does not require any form of coordination, data sharing, or synchronization. As a result, any two devices can be localized with respect to each other even without establishing a two-way communication. In this paper, we exploit *multipath triangulation* with WiFi to develop a device-based localization system called *MonoLoco* and show that this technique even works on commodity WiFi devices. MonoLoco is a system that provides decimeter level location and orientation information using just a single unaided WiFi receiver. it defines a novel 3-dimensional super-resolution algorithm that leverages CSI measurements to estimate the geometric features of multipath reflections, and builds upon previous Joint AoA and Delay Estimation (JADE) techniques [18, 37, 39]. Table 1 summarizes how MonoLoco compares with existing WiFi-based localization systems.

Disentangling multipath is a widely studied problem in ToF cameras [25], light imaging [10, 13], or wireless sensing and imaging[1, 3, 36, 37]. A recent system called WiCapture [19] introduces a WiFi-based technique for motion tracking that uses multipath reflections to compensate for the distortions caused by the sampling frequency offset. So, it can estimate the trajectory of the motion (not the absolute position of the target) by using the temporal changes in the phase of the received signal in multiple WiFi access points. Unlike this previous system, *multipath triangulation* directly uses multipath reflections for geometric mapping in place of multiple nodes to perform triangulation.

Besides localizing another device, prior works have also attempted other forms of localization such as device-free localization of a person with FMCW radars [2, 3], UWB impulse radars [15, 53], RFID [44], or WiFi [6, 43], as well as self-localization of a target/robot in the environment with fingerprinting [5, 8, 21, 34, 52, 52], ambient signals [12], SLAM-based techniques [30], or dead reckoning [38]. These techniques are complementary to our system where every wireless node can localize other nodes with respect to itself.

Orientation Estimation: The standard way to measure the orientation of a device is via the use of IMUs [14, 16]. However, with

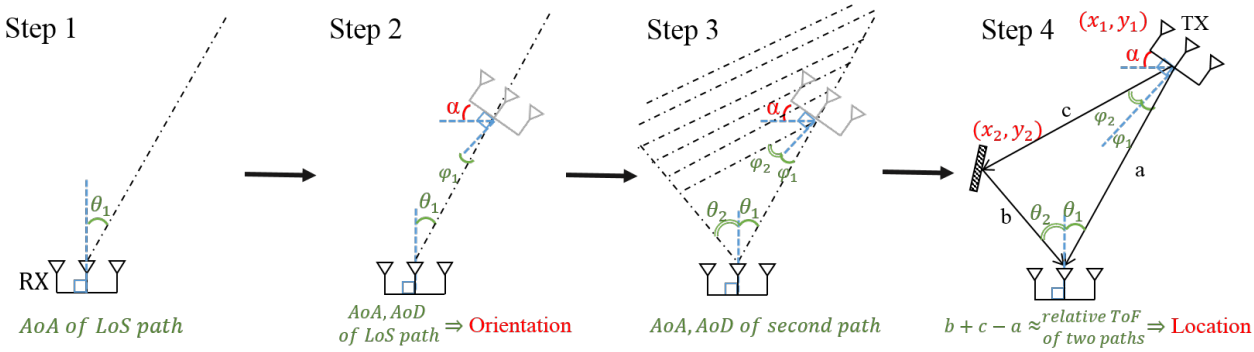

Figure 1: Multipath triangulation uses the (1) AoA and (2) AoD of the direct path to estimate the target's orientation. Then, in step (3), it uses AoA and AoD of the reflected path to find the relative location of the target with respect to the reflector and the receiver. In step (4), it uses the relative ToF between the two paths to find the target location.

IMUs, the gyroscope only provides the derivative of the yaw while the magnetometer can be limited by perturbation in measuring the heading in indoor spaces [4]. As a result, some wireless-based solutions are introduced [26, 35], which use MIMO to estimate AoA and AoD. However, the performance of these methods is limited by coarse-grained multipath resolution. *Multipath triangulation* uses the same principle but applies a 3-dimensional super-resolution algorithm to extract the features of multipath more accurately and identify the direct path from which the orientation is estimated.

3 MULTIPATH TRIANGULATION

Conventional features of multipath reflections such as AoA, AoD, and ToF are determined in large part by the location of the reflection surface, which is neither known nor of interest. These multipath features do not contain any information about the relationship of the receiver and the transmitter locations. As such, multipath reflections have generally not been considered useful for localization. In this paper, we introduce a new geometric algorithm called *multipath triangulation* that combines the geometric features of a multipath reflection with the LoS path to estimate the location and orientation of the target device as well as the location of the reflector. The basic insight behind *multipath triangulation* is that the *relative* ToF (rToF) of two paths, the difference between the length of the reflected path and the direct path, actually does have useful information even while the *absolute* ToF of a multipath reflection does not. The direct path and a reflected path form a triangle with the AP at one vertex, the target at another vertex, and the reflection surface at the third vertex. Two angles of that triangle can be known based on the AoA and AoD of the two paths, and the rToF constrains the relative lengths of the sides of the triangle. Together, these constraints fully determine the triangle and thus the location of the target and the reflector.

More concretely, the following 4-step procedure can determine the location/orientation of the target, as illustrated in Figure 1. In step (1), the AoA of the direct path (θ_1) constrains the target location to be on line relative to the orientation of the receiver's antenna array. In step (2), the AoD of the direct path (φ_1) constrains the orientation of the target's antenna array with respect to the receiver's antenna array. This orientation is labeled α. In step (3), the AoA and AoD of the reflected path (θ_2 and φ_2) define a triangle between the target, the receiver, and the reflector, but the size of that triangle is still unconstrained. Here, the key innovation of *multipath triangulation* comes into play. From all possible triangles, only one of them has the corresponding rToF (i.e. the ToF difference of the reflected path and the direct path). Therefore, in step (4), the rToF (ΔT) constrains the size of the triangle such that $b + c - a = \Delta T \times C$, where $b + c$ is the length of the reflected path, a is length of the direct path, and C is the speed of light. This fully determines the triangle, allowing the location of the target (x_1,y_1) and the location of the target (x_2,y_2) to be known.

Conventional triangulation method fully determines the triangle formed by a target and two receivers by using three pieces of information: two AoA estimates from the target to the receivers, and the distance between the reference receivers. This method is based on the classical angle-side-angle triangle congruence theorem which proves that these three properties are sufficient to fully determine any triangle. *Multipath triangulation* uses a similar process to fully determine the triangle formed by multipath reflections, except that it uses four angle estimates (AoA and AoD of the direct path and a reflected path) and one rToF value.

It should be noted that the principles of *multipath triangulation* are independent of the frequency of the RF signal, antenna array arrangement, or the multipath resolution algorithm. In addition, this new triangulation algorithm can be used for different types of applications where the location or orientation of another device or a reflector is of interest. These applications range from indoor navigation and mapping to health/elderly monitoring. In this paper, we focus on device-based localization and show that this approach even works on commodity WiFi devices by using MIMO-OFDM technology and only 3 antennas. We use *multipath triangulation* to localize two WiFi devices with respect to each other. This results into *MonoLoco*, the first decimeter-level WiFi localization system that requires no coordination, data sharing or even two-way communication between the transmitter and receiver. In the next section, we explain the details of *MonoLoco* and the implementation of *multipath triangulation* for device-based localization.

4 MONOLOCO: DEVICE LOCALIZATION

Commodity WiFi chips provide the amplitude and phase shifts introduced by the wireless channel in the format of Channel State Information (CSI). MonoLoco exploits *multipath triangulation* algorithm and CSI values from a 3-element antenna array and 30 frequency subcarriers to localize and orient another WiFi device. In this section, we first explain how MonoLoco estimates the geometric features of multipaths such as AoA, AoD, and ToF. Then, we detail the implementation of the localization algorithm derived from *multipath triangulation*. Finally, we explain how MonoLoco deals with antenna array symmetry and improves localization using multiple packets, if they are available.

4.1 Super-resolution of AoA, AoD, and ToF

MonoLoco uses a new method to resolve the AoA, AoD, and ToF of multiple propagation paths between the transmitter and receiver. The basic intuition is that (a) the AoA creates a predictable phase shift on the different sensing elements of the receiving antenna array, (b) the AoD creates a predictable phase shift from each of the transmitting antennas on a given receiving element, and (c) the ToF creates a predictable phase shift across different frequencies. To calculate these values, MonoLoco combines measurements across multiple subcarriers on multiple receiving antennas, from each of the transmitting antennas. In our implementation, we use 3 receiving antennas, 3 transmitting antennas, and 30 subcarriers for a total of 270 sensing elements. In theory, this large aperture could resolve as many as 269 different propagation paths. In practice, however, only a handful of paths can be resolved due to measurement noises. Still, this set of 270 sensing elements contains enough information to estimate the AoA, AoD, and ToF and the large aperture allows for a higher accuracy than state of the art methods. Implementations that use more antenna elements or more frequencies could achieve even higher accuracy.

Given this sensing array, MonoLoco resolves multipath features using a joint estimation technique that we call *3-dimensional super-resolution*. This approach builds on well-established noise subspace methods such as MUSIC [33] and Joint AoA and Delay Estimation (JADE) techniques [18, 39]. We first explain how the standard MUSIC algorithm works, and then present our extensions for joint estimation of AoA, AoD, and ToF.

4.1.1 ***MUSIC Overview.*** MUSIC is based on the intuition that when different propagation paths have different AoAs, the paths can be resolved by leveraging the extra phase shift introduced by the paths on the antenna array. As shown in Figure 2, this additional phase shift is due to the extra distance that the signal travels to reach the succeeding elements of the antenna array. This added phase shift $\Phi(\theta_l)$ is a function of both the AoA of that path and the distance between antennas, and can be expressed as:

$$\Phi(\theta_l) = e^{-j2\pi f d \sin(\theta_l)/C} \tag{1}$$

where θ_l is the AoA of the l^{th} path, d is the distance between the antennas, C is the speed of light, and f is the frequency of the transmitted signal. Consequently, the resulting vector of received signals across the antenna array due to l^{th} path can be written as a linear combination of the signal incident on the first (reference) antenna as:

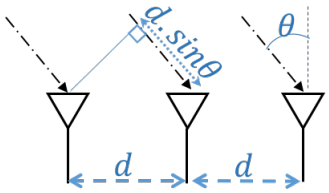

Figure 2: The phase shift across the antenna array is a function of the antenna spacing d and the angle of arrival θ of the signal.

$$X(t) = [x_1(t), ..., x_M(t)]^T = a(\theta)s(t) + N(t) \tag{2}$$

where M is the number of receiving antennas, $s(t)$ is the received signal at the first antenna and $N(t)$ is the noise vector. $a(\theta)$ is called the *steering vector* and expresses the expected phase differences across the antenna array:

$$a(\theta) = [1, \Phi(\theta)^1, ..., \Phi(\theta)^{M-1}]^T \tag{3}$$

When there are L incident paths arriving at the antenna array, the signal received at each antenna is the superposition of all paths. Therefore, Equation 2 can be written as

$$X(t) = \sum_{i=1}^{L} a(\theta_i)s_i(t) + N(t) \tag{4}$$

The MUSIC algorithm analyzes the eigen structure of the correlation matrix by defining $M - L$ eigenvalues as the noise subspace $E_L = [e_1, ..., e_{M-L}]$ and the other L eigenvalues as the signal subspace. Then, it searches for the AoAs whose steering vectors are orthogonal to the noise subspace, which appear as peaks in the following spatial spectrum function:

$$P(\theta) = \frac{1}{a^H(\theta)E_L E_L^H a(\theta)} \tag{5}$$

4.1.2 ***3D Super-resolution.*** We extend the standard MUSIC algorithm into a 3 dimensional joint estimation by leveraging the spatial diversity in receiving antenna array to estimate AoA, the spatial diversity in transmitting antenna array to estimate AoD, and frequency diversity across OFDM subcarriers to estimate relative ToF. The signal emitted from a linear transmit array will be received with a phase shift $\Gamma(\varphi)$, which is function of AoD. For l^{th} path with AoD φ_l, the phase shift across transmitting antennas is given by:

$$\Gamma(\varphi_l) = e^{-j2\pi f d' \sin(\varphi_l)/C} \tag{6}$$

where d' is the distance between transmitting antennas.

Furthermore, the current WiFi standards such as 802.11 leverage OFDM technology wherein data is transmitted over multiple subcarriers. For equispaced OFDM subcarriers, the l^{th} path with ToF of τ_l introduces a phase shift of

$$\Omega(\tau_l) = e^{-j2\pi f_\delta T_l} \tag{7}$$

across two consecutive OFDM subcarriers with f_δ frequency difference. We point out that the phase shifts due to AoA and AoD across

subcarriers are negligible due to the small frequency difference across WiFi channels [18].

MonoLoco jointly estimates AoA, AoD, and ToF by defining the sensor array from all subcarriers of all receiving antennas for all streams transmitted from multiple antennas. This information is accessible in commodity WiFi chips with MIMO-OFDM techniques (more specifically MIMO spatial multiplexing). The overall attenuation and phase shift introduced by the channel measured at each subcarrier by each antenna is reported as the *Channel State Information* (CSI) in a 3×3×30 format - 3 receiving antennas, 3 transmitting antennas, and 30 subcarriers. Therefore, the measured sensor array X is constructed by stacking CSI from all the subcarriers at all antennas, resulting in a single column vector of length $3 \times 3 \times 30$ (= 270). The new steering vector $a(\theta, \varphi, \tau)$ is formed by phase shifts introduced at each of the sensors, and is given by:

$$a'(\theta, \tau) = [\overbrace{1..\Omega_\tau^{K-1}}^{RX_1}, \underbrace{\Phi_\theta, \ldots, \Omega_\tau^{K-1}\Phi_\theta}_{RX_2}, \ldots, \overbrace{\Phi_\theta^{M-1}, \ldots, \Omega_\tau^{K-1}\Phi_\theta^{M-1}}^{RX_M}]^T \tag{8}$$

$$a(\theta, \varphi, \tau) = [a'_{\theta,\tau}, \Gamma_\varphi a'_{\theta,\tau}, ..., \Gamma_\varphi^{N-1} a'_{\theta,\tau}]^T \tag{9}$$

where $\Omega(\tau)$ is written as Ω_τ, $\Phi(\theta)$ as Φ_θ, and $\Gamma(\varphi)$ is written as Γ_φ. Therefore, the new measurement matrix X is constructed using the above steering vector, and three parameters of AoA, AoD, and ToF that maximize the spatial spectrum function (Equation 5) will be estimated. However, this requires finding the peaks in a 4D space $(\theta, \varphi, \tau, P)$. To solve this problem, instead of implementing the standard MUSIC algorithm, we use the improved version called RAP-MUSIC [29], which uses an iterative mechanism to find the paths from signal subspace instead of noise subspace. Therefore, in each iteration, the global maximum is considered as the resolved path.

Another challenging issue is that the ToF estimates do not capture the actual time that the signal travels. The reason is that the WiFi transmitter and receiver are not time-synchronized. Furthermore, the estimated ToFs also include the delays from sampling time offset and packet detection delay [18, 34]. To address this challenge, in the next section, we explain MonoLoco's ToF sanitization approach, which results in accurate estimation of the relative ToF between different resolved paths.

4.1.3 ***ToF Sanitization.*** One of the challenges in estimating ToF with commodity WiFi devices is that the measured channel at the receiver experiences a random phase shift due to sampling time offset (STO) and packet detection delay (PDD) across packets [34]. While the variations due to sampling time offset may seem small, packet detection delays are often an order of magnitude larger than ToF [40]. To address this challenge, MonoLoco applies a ToF sanitization algorithm similar to the ones proposed in PinLoc [34] and SpotFi [18].

STO and PDD have a constant effect across all transmitting (TX) or receiving (RX) antennas since all the radio chains of a WiFi card are time-synchronized. Hence, an additional delay of τ_s adds a phase shift of $-2\pi f_\delta(k-1)\tau_s$ to the phase of the k^{th} subcarrier in each antenna. For each CSI measurement, we remove the offset by removing the linear fit of the unwrapped phase shifts across subcarriers of all $N \times M$ antennas. Suppose $\psi(n, m, k)$ is the unwrapped phase of the CSI at the k^{th} subcarrier of a packet transmitted from the n^{th} TX antenna and received at the m^{th} RX antenna, then we can obtain the optimal linear fit as:

$$\hat{\tau_s} = arg\min_{\beta} \sum_{n,m=1}^{N,M} \sum_{k=1}^{K} (\psi(n, m, k) + 2\pi f_\delta(k-1)\beta + \alpha)^2 \tag{10}$$

Intuitively, β is the common slope of the received phase responses for all antennas, and α is the offset. The modified CSI phase is then defined to be:

$$\hat{\psi}(n, m, k) = \psi(n, m, k) - 2\pi f_\delta(k-1)\hat{\tau_s} \tag{11}$$

Note that this technique does not estimate the exact value of τ_s for each packet. The slope of unwrapped phases across the subcarriers consists of the delay caused by STO/PDD as well as the phase shift due to ToF of the shortest path. Therefore, subtracting this value leaves only enough information to derive the *relative* ToF (rToF) between multipaths. In other words, the values τ_l derived in Section 4.1.2 are not valid after ToF sanitation, but the rToF value $\Delta T_j = \tau_j - \tau_1$ for path $j > 1$ with respect to the shortest path is still valid.

4.2 Localizing the Target

MonoLoco localizes the target by combining the resolved geometric features of multipaths described above: the AoA and AoD of multiple propagation paths, and the rToF between the LoS path and each reflected path. MonoLoco defines the LoS path to be the resolved path with the shortest ToF value. To localize, MonoLoco finds the orientation and location of the target that best explains these observed multipath features, as described below.

4.2.1 ***Multipath Geometry.*** Without loss of generality, we explain MonoLoco's multipath geometry in a simple case of two paths; but the method generalizes to more multipath signals in a straightforward manner. Figure 3 illustrates an example of the target location and orientation. The path angles are defined to vary between $-\frac{\pi}{2}$ to $\frac{\pi}{2}$ going from the 3rd array element to the 1st, as illustrated. In the example in the figure, the LoS signal is transmitted from the target with AoD φ_1, propagates a distance a and arrives at the receiver with AoA θ_1. The multipath reflection is transmitted from the target with AoD φ_2, propagates a distance $b + c$ and arrives at the receiver with AoA θ_2. These values represent the 5 multipath features resolved by the signal processing algorithms in Section 4.1: AoA (θ_1) and AoD (φ_1) of the LoS path, AoA (θ_2) and AoD (φ_2) of the reflected path, and the relative ToF between two paths $\Delta T = \tau_2 - \tau_1$.

Given these values, MonoLoco must estimate 5 new parameters: the target orientation (α), the target location (x_1, y_1), and the reflector location (x_2, y_2). We define the coordinate system with respect to the receiver's antenna array and the orientation of the target α is defined to vary between 0 to 2π moving clockwise. With these definitions, the multipath geometry defines four triangles named $\mathbb{A} - \mathbb{D}$, as shown in Figure 3. We use these triangles to define the following 4 equations that relate the observed multipath features to

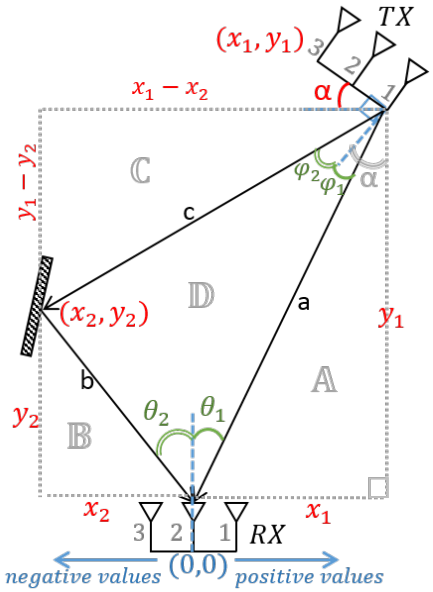

Figure 3: Multipath Geometry. The direct path and a multipath reflection form a triangle (𝔻) between the AP, the target, and the reflector. This triangle defines a relationship between the target location/orientation and the observed AoA, AoD, and rToF values. That relationship can be encoded in terms of three other triangles (𝔸, 𝔹, and ℂ).

the location and orientation parameters we are trying to estimate:

$$\triangle\mathbb{A}: \frac{x_1}{y_1} = \tan(\theta_1) \tag{12}$$

$$\triangle\mathbb{B}: \frac{x_2}{y_2} = \tan(\theta_2)$$

$$\triangle\mathbb{C}: \frac{x_1 - x_2}{y_1 - y_2} = \tan(\alpha - \varphi_2), \text{ where}$$

$$\alpha = \varphi_1 + \theta_1$$

$$\triangle\mathbb{D}: b + c - a = \Delta T \times C, \text{ where}$$

$$a = \|x_1, y_1\|_2$$

$$b = \|x_2, y_2\|_2$$

$$c = \|(x_1 - x_2), (y_1 - y_2)\|_2$$

where C is the speed of light. Intuitively, equations derived from triangles $\mathbb{A}$ to $\mathbb{C}$ define the relative location of the target with respect to the receiver and the reflector. The equation derived from triangle $\mathbb{D}$ leverages the relative ToF to define the actual scale of these triangles since there is only one scale that satisfies $b+c-a = \Delta T \times C$. Finally, the orientation of the target is defined to be

$$\alpha = \varphi_1 + \theta_1 \tag{13}$$

MonoLoco solves for α directly using the equation above and solves for the location parameters $XY = [\hat{x_1}, \hat{y_1}, \hat{x_2}, \hat{y_2}]$ by solving the following non-linear optimization problem:

$$[\hat{XY}] = \underset{XY}{\text{argmin}}\ S(XY) \tag{14}$$

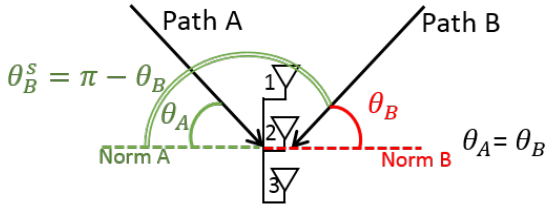

Figure 4: The symmetry of a linear antenna array creates ambiguity in AoA and AoD measurements. Therefore, MonoLoco solves for the target location that best explains either the resolved angle or its supplementary angle.

where

$$S(XY) = [\tan(\theta_1) - \frac{x_1}{y_1}]^2 + [\tan(\theta_2) - \frac{x_2}{y_2}]^2 + [\tan(\alpha - \varphi_2) - \frac{x_1 - x_2}{y_1 - y_2}]^2 + [(\Delta T \times C) - (b + c - a)]^2$$

To optimize this objective function, we search for the most likely location of the target and reflector by forming a 20 centimeter by 20 centimeter grid, and evaluating $S(XY)$ at each point in the grid. Then, we use constrained nonlinear optimization (the fmincon solver in Matlab) on the three positions with minimum $S(XY)$ in the grid to find the best solution.

Note that the above equations will hold for any arrangement of target-reflector location and orientation, and could be applied to different antenna array arrangements. We will discuss symmetry ambiguity of linear arrays in Section 4.2.2 and explain the required modifications to provide 360-degree coverage.

4.2.2 ***Overcoming Antenna Symmetry.*** The angle spectrum resolved with a linear antenna array is 180 degrees, so it cannot determine from which side of the array the signal is arriving. Figure 4 illustrates an example of this ambiguity in which incident paths A and B arrive from different sides of the array but the observed AoA for the two paths are equal ($\theta_A = \theta_B$). The reason for the angle ambiguity is that a linear array has reflectional symmetry along the direction of the array, and so signals from both sides produce equivalent phase shifts across a linear antenna array.

In many applications such as robotics and virtual reality where WiFi devices can be anywhere in the surrounding environment, a circular or non-linear array is used to break this symmetry by adding a sensing element in a second dimension, thereby increasing the angle resolution to a full 360 degrees. However, most commercial APs still use linear antenna arrays and so, in this paper, we evaluate MonoLoco using linear antenna arrays. This is a worst-case analysis and future products that can be built with circular arrays can achieve higher accuracy.

Given this symmetry, any AoA (or AoD) value θ could actually be one of two possible values: θ or $\pi - \theta$. To address this challenge, MonoLoco applies the localization algorithm using both the resolved angle and its supplementary angle. Therefore, it runs 8 optimization processes in parallel to examine the symmetry ambiguity for the AoA and AoD of the reflected path and AoD of the direct path (e.i. 3 slots with 2 possible values for each result in 8 combinations or 8 symmetry scenarios). Then, from 8 estimated

locations, MonoLoco chooses the one with minimum cost value of the objective function in the corresponding estimated location. The intuition behind this algorithm is that only one of these 8 conditions is geometrically feasible, which appears with minimum cost value. It should be noted that this approach is not a solution for identifying the symmetry scenario, but just a mechanism to estimate the location and orientation of the target regardless of the symmetry ambiguity. We expect to have errors in estimating the correct symmetry scenario in the case of large errors in multipath resolution, but eventually, we expect that the final estimated location is the best solution since it has the minimum cost value.

4.2.3 ***Improving Localization using Multiple Packets.*** Every packet that is received creates a new observation of the 5 resolved multipath features described above. If more than one packet is received, these observations can be combined to create an over-constrained system of non-linear equations in order to further improve localization. There are many ways to solve this non-linear system and in this section we describe a 3-step data cleaning process. This process is motivated by our observation that noise in some packets can cause super-resolution to resolve spurious paths, while other packets resolve correct paths. The three steps are described below.

Step 1: We estimate the location/orientation parameters for each packet independently, using the methods described before. Any packet with spurious paths will generally result in geometrically infeasible conditions, which will manifest as high values of the objective function $S(XY)$. Therefore, MonoLoco uses a very low threshold value to discard any packets with objective values substantially higher than zero. Note that any packet with geometrically feasible multipath features will have an objective value that is close to zero, so this step does not eliminate all packets with errors.

Step 2: Previously, we assumed the path with the shortest ToF is the direct path. However, in the presence of spurious resolved paths, this assumption may not be held. To this end, Multipath features from the remaining packets are used to determine the true LoS path. MonoLoco applies the K-means clustering algorithm on all paths from remaining packets. The number of clusters is set to 5, based on the typical number of dominant paths in an indoor environment [9, 47]. Then, we extend the SpotFi's direct path likelihood function [18], where the likelihood of l^{th} path being the direct path is calculated as

$$P_l = exp(\omega_C \bar{C}_l - \omega_\theta \bar{\sigma}_{\theta_l} - \omega_\varphi \bar{\sigma}_{\varphi_l} - \omega_\tau \bar{\sigma}_{\tau_l} - \omega_s \bar{\tau}_l) \quad (15)$$

where $\bar{C}_l$ is the number of points in the cluster of l^{th} path, $\bar{\tau}_l$ is the average ToF of the cluster, and $\bar{\sigma}_{\theta_l}$, $\bar{\sigma}_{\varphi_l}$, and $\bar{\sigma}_{\tau_l}$ are the population variances of the estimated AoAs, AoDs, and ToFs for the corresponding cluster, respectively. The ω weighting factors are constant values to account for different scales of the corresponding terms [18]. The intuition behind this approach is that the parameters of the direct path have small variations over time compared to the estimated reflected paths. Therefore, the size and variance of each cluster are strong indicators of the LoS path.

After the true LoS path is identified, MonoLoco filters any remaining packets that have a resolved path that is shorter than the LoS path. In other words, it recalculates the rToF between the reflected path and the LoS path and filters out the packets where the identified direct path does not have the shortest ToF:

$$\exists\ \tau_i^{ref} \mid (\tau_i^{los} - \tau_i^{ref}) < 0 \quad (16)$$

where τ_i^{los} and τ_i^{ref} are the ToF of the direct path and the reflected path in i^{th} packet, respectively.

Step 3: The set of remaining packets is called ($P_{filtered}$), each of which has its own location/orientation estimate. MonoLoco chooses the packet that has the lowest objective value. This could be expressed as

$$[\hat{XY}, \hat{\alpha}] = \arg\min_{XY_i} S(XY_i),\ i \in P_{filtered} \quad (17)$$

Intuitively, MonoLoco chooses the packet for which the 5 resolved multipath features are most consistent with each other, presumably because this packet was subject to the least noise. We did not do a comprehensive exploration of the selection algorithm and present this one only as a proof of concept. We believe that other approaches to solve full non-linear system defined by $P_{filtered}$ may indeed produce better results.

5 EVALUATION

5.1 Experimental Setup

We evaluate our system using Intel NUCs D54250WYK[1] equipped with off-the-shelf Intel 5300 WiFi cards which support three antennas. We employed Linux CSI tool [11] to obtain the PHY layer CSI information for each packet. The experiments are conducted in the 5 GHz WiFi spectrum using 40 MHz bandwidth. We built 9 nodes and used one node as the access point (AP) and 8 nodes as target devices in multiple locations (as illustrated in Figure 5). We use the method introduced in WiCapture [17, 19] for calibration and operated all nodes in monitor mode. Each node was equipped with three 3dBi omni-directional antennas[2] in a uniform linear array. The distance between any two antennas is equal to 2.7 cm (half a wavelength). The nodes were placed atop 110cm speaker stands during the experiments to represent a practical height.

All experiments were conducted as follows. First, all nodes (both AP and target nodes) are set in monitor mode on channel 118 with 40 MHz bandwidth in the 5GHz band. Then, for every target location shown in the testbeds, 500 packets were transmitted with a 5 ms interval using the spatial multiplexing protocol in 802.11n. Measurements were collected in both directions – from the target to the AP and from the AP to the target – both of which were analyzed independently as separate experiments to estimate the location of one device with respect to the other one. The main results are calculated using 20 packets and the impact of the number of packets on localization is discussed in Section 6.3.

We first validate the localization model in an anechoic chamber as shown in Figure 6(a). This enabled experiments with known propagation paths. The number of reflections was varied between 1 to 5 and different orientations and positions were measured, resulting in 30 different target positions in total, as shown in Figure 5(a). Then, to evaluate the performance of MonoLoco in more realistic conditions, we deployed in a home with two occupants, in two

[1] https://ark.intel.com/products/76977/Intel-NUC-Kit-D54250WYK
[2] https://www.data-alliance.net/antenna-5-1-5-8ghz-3dbi-omni-directional-dipole-w-rp-sma-male-connector/

Figure 5: Experiments were run in four environments with varying size and multipath complexity. The closest AP to each target was used for localization.

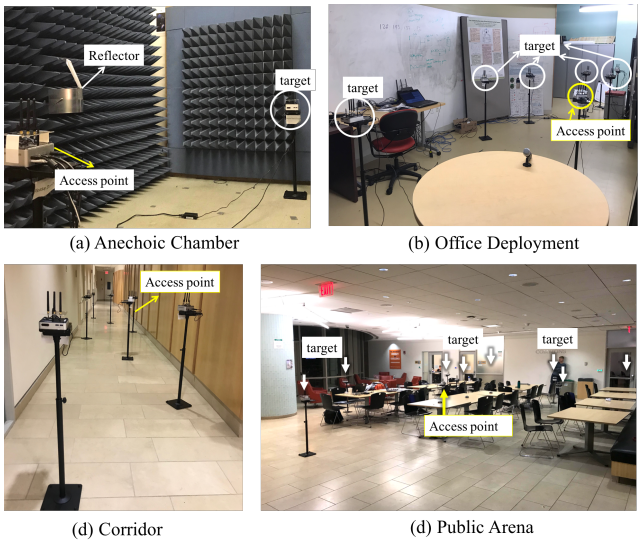

Figure 6: The four experiments tested different distances, angles, and multipath environments.

offices environments and a large public arena with the presence of 1-5 occupants. Locations of WiFi APs and 51 target locations are depicted in Figures 5(b)-(d) with the snapshots of the deployment environments in 6(b)-(d). These experiments resulted in 102 different experimental scenarios, including both directions (from AP to target and target to AP). In cases where more than one AP is deployed to span the area, the closest AP to the target location was used for localization. The majority of node distances are between $1m$ to $4m$ due to the size of the spaces available, but 26% of total experiments evaluate distances larger than $4m$ especially in the corridor and public arena. This is similar to the experimental setup of the related works [40, 47] with 25-35% of localization tests having $4m$ to $15m$ distances. Ground truth location and orientation were measured using a combination of laser range finder, a construction protractor, floor and ceiling tiles, and architectural drawings of the building.

We compare the performance of the proposed 3D super-resolution algorithm with the 2D method proposed in Spotfi [18]. However, the closest available localization system to MonoLoco is Chronos [40] that demonstrates accurate WiFi localization with a single AP, but it relies on external coordination between the transmitter and receiver for sharing channel measurements in each side of transmission as well as frequency hopping. In contrast, MonoLoco assumes no coordination or data sharing between the two nodes. In addition, Chronos requires a large spacing in the AP's antenna array (12-30cm) and so it would be severely handicapped if run on the hardware designed for MonoLoco. So a head-to-head comparison would not be meaningful and only a qualitative comparison is provided.

5.2 Model Validation in Anechoic Chamber

Before testing in a realistic environment, we validated the proposed localization model in a controlled environment such as an anechoic chamber with known propagation paths. This experiment establishes an experimental upper bound on accuracy by limiting multipath reflections. We first established the lack of multipath reflections in the anechoic chamber by verifying that no packets are received since the spatial multiplexing technique in 802.11n requires multipath propagation to make multi-stream transmissions. Any reflections in the chamber were not strong enough to enable transmission. Then, we placed 1-5 curved metal sheets at different locations in the chamber to generate controlled multipath geometries. These geometries included the ambiguity caused by antenna symmetry described in Section 4.2.2. The metal sheets were curved to create a scattering effect, increasing the chance that the reflections reach the receiver. We used packet reception rate to verify the incidence of at least one reflection path.

From Figure 7, we observe that the proposed localization method achieves a median localization error of $25cm$ and median orienting error of 3.5 degrees in anechoic chamber. There are likely two main sources of this error. First, ground truth: since the coordinate system is defined relative to the AP antenna orientation, ground truth errors can produce error in target location. Second, multipath resolution: the resolution capability of MUSIC is limited by the angular separation of multipath components, and the physical geometry of the linear antenna arrays causes lower resolution of estimated angles as they approach their extremes ($-pi/2$ and $pi/2$) [47].

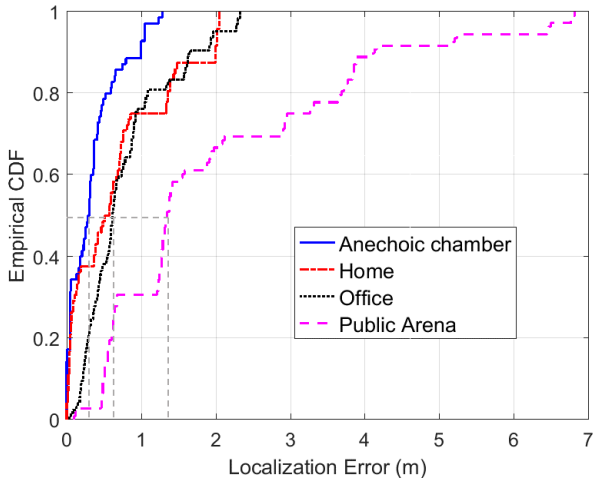

Figure 7: The cumulative distribution of location error shows that MonoLoco's median error varies between $0.2m$ to $1.3m$ across environments with different multipath complexity.

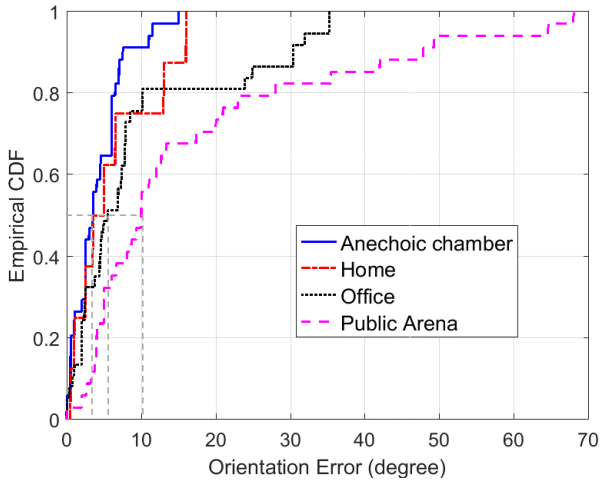

Figure 8: The cumulative distribution of orientation error shows that the median error varies between 3.5 to 10 degrees across environments with different multipath complexity.

5.3 Location Accuracy

Next, we evaluate MonoLoco in realistic indoor environments with complex multipath propagation. We deploy multiple WiFi nodes equipped with WiFi cards in three sets of environment with different levels of complexity: (1) a home deployment, which is a cluttered environment with a lot of furniture nearby the nodes; (2) two office environments, which includes deployment in two offices on two sides of a corridor. During the experiment there were 1 to 5 occupants inside the offices sitting at the desks, and (3) two public areas, including a large open space and two corridors. The open space area contained many tables and chairs at about the same height as the WiFi nodes, which resulted in a complex multipath environment and NLoS scenarios. Both areas enabled larger distances between the AP and the targets, compared to the home and office deployment. The open area allowed reflection paths that were much longer than the LoS signal while the corridors were narrow and limited the separation of propagated paths from the LoS signal.

As seen from Figure 7, the median localization error of MonoLoco is $0.54m$ and $0.64m$ in home and office deployments, respectively. Under stressful conditions in the public arena deployment, the median localization error approaches $1.3m$ which is proportional to the distance of the links. The higher error rate in this area is due to rich multipath propagation and lower resolution of multipath estimates. In addition, the public arena deployment contains NLoS conditions due to obstacles in the LoS path such as furniture and glass walls. We point out that the reception of direct path is essential for MonoLoco's localization algorithm, but the results show that it is robust to partial LoS blockage. These results show that MonoLoco's accuracy is comparable to state-of-the-art indoor localization systems that use multiple APs [18, 22, 47], or frequency hopping for ToF measurements [27, 40].

5.4 Orientation Accuracy

Besides localization, MonoLoco provides the orientation information. In the experiments performed in four environments shown in Figure 5, random orientations are chosen for each target location ranging between 0 to 2π. As seen in Figure 8, MonoLoco achieves a median orientation error of 3.5 degrees in anechoic chamber, 4.2 degrees in home, 5.5 degrees in office deployments, and 10 degrees in public arena deployment. The main reason for MonoLoco's high performance in estimation of the orientation is that orientation is mainly derived from AoA and AoD of the direct path, which is the dominant component in the received signal, and therefore less prone to multipath resolution error.

MonoLoco achieves high accuracy in estimating location and orientation for two main reasons. First, MonoLoco's multipath super-resolution algorithm resolves multipath components more accurately by using a 3D joint estimation. Second, MonoLoco jointly computes the location and orientation by minimizing the geometric errors along multiple paths. Therefore, identifying the orientation allows to compensate the errors in localization estimation.

6 SENSITIVITY ANALYSIS

6.1 AoA-AoD Estimation Accuracy

The goal here is to show that MonoLoco's 3D super-resolution algorithm provides a more accurate AoA and AoD estimation than state of the art. However, we don't have the ground truth parameters of the reflection paths in the realistic environments. Therefore, in Figure 9, we show the accuracy of the AoA and AoD estimations only for the direct path. After running the super-resolution algorithm, we choose the resolved AoA and AoD values that are closest to the LoS path and calculate their difference from the ground truth values. We compare this error with the 2D AoA-ToF estimation method proposed in SpotFi [18]. To measure AoD with SpotFi, it is applied on transmitting antenna array incident on the first receiving antenna.

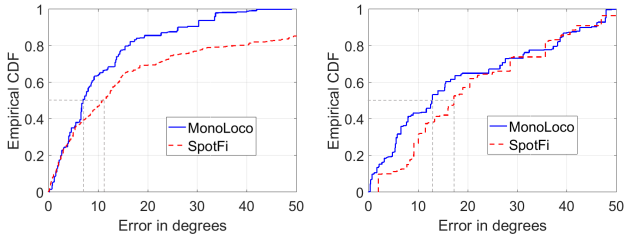

(a) AoA Estimation error (b) AoD estimation error

Figure 9: MonoLoco's 3D super-resolution algorithm improves both (a) AoA and (b) AoD estimation in comparison with SpotFi's 2D approach [18].

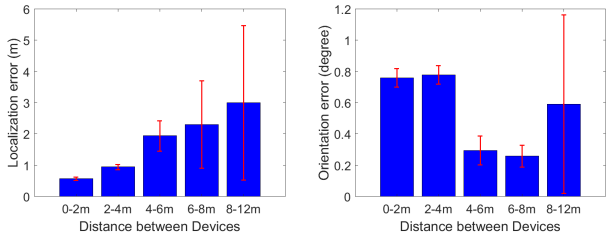

(a) (b)

Figure 10: The average (a) localization, and (b) orientation errors increase as the distance between the target location and the AP increases.

Figure 9(a) plots the CDFs for AoA estimation error for all links in all experiments. MonoLoco achieves median AoA accuracy of 4.02 degrees better than that achieved by SpotFi. In AoD estimation, shown in Figure 9(b), MonoLoco achieves an improvement of 4.53 degrees in the direct path error. The reason for the higher performance of MonoLoco compared to SpotFi is that a larger sensor array consisting of 3 transmitting antenna, 3 receiving antenna, and 30 subcarriers ($3 \times 3 \times 30 = 270$) is used, which provides larger aperture to separate multipath components. In addition, in AoD estimation, both methods converge to similar error rates in 80^{th} percentile of the error. This is more a limitation of the linear antenna array; any method will produce higher error when the incident angle of the signal approaches the angle of the array.

6.2 Impact of Distance

Next, we evaluate the impact of the distance between two transceivers on location and orientation accuracy. Figure 10 plots the distance between each target location and the AP against localization and orientation error in the 4 deployments. In Figure 10(a), we observe that the average localization error increases with the increase of the distance between two nodes. This is primarily due to the reduced signal-to-noise ratio at greater distances, which results in lower accuracy in multipath resolution (especially for reflected paths). In addition, the majority of target locations with long distances belong to the public arena deployment which is a cluttered environment with narrow corridors and complex multipath propagation.

It should be noted that the population of the experimental locations is not uniform across different distances with a lower density around large distances ($> 5m$). This imbalance is taken into account in calculation of 90%-percentile confidence intervals, which appeared as an increasing pattern across distances. On the other hand, the localization accuracy is provided for each environment separately in Figure 7 since the distribution of link distances are not uniform in all experimental environments. In Anechoic chamber where link distances are between $0.85m$ to $2.7m$, the median localization error is $25cm$. In home and office environment with link distances between $1.1m$ to $5.5m$, the location error is $0.54m$ to $0.64m$. Finally, in the public arena with link sizes between $1.5m$ to $12.7m$, the median accuracy is $1.3m$. Therefore, we can conclude that the accuracy is proportional to the distance of the nodes.

Figure 10(b) shows the orientation accuracy against the distance between each target location and the AP. Although it is expected that the average orientation error increases with an increase in distance, our observations show the distance is not the main factor in the accuracy of orientation estimates. The reason is that orientation is mainly calculated from the AoA and AoD of the direct path which carries the dominant signal power, thus less prone to the additional noises from further distances. Theoretically, the accuracy of the resolved angles is the main factor affecting the orientation estimation. The resolution of subspace methods such as MUSIC degrades as the incident angles approach the edges of the spectrum (e.g. $-\pi$ and π in linear antenna arrays). Therefore, for a linear antenna arrangement, the accuracy of the orientation estimation would be lower if the target's antenna array is either perpendicular or in-line to the AP's array.

6.3 Impact of Number of Packets

Section 4.2.3 describes how MonoLoco combines data from multiple packets, if available. Figure 11 shows how this approach affects localization accuracy as the number of packets used for localization is changed from 7 packets to 50 packets. Each line represents the cumulative distribution of the combined error in all four environments for a given number of packets. Even with 7 packets, MonoLoco achieves a median localization accuracy of $0.84m$ using all deployments including the public arena, compared to $0.5m$ obtained using 50 packets. With only 1 packet, it was able to achieve $0.7m$ error in the home and offices and approximately $2m$ error in the public arena. These results indicate that MonoLoco is able to achieve location estimates with reasonable accuracy with only the first few packets, and gets diminishing returns as more packets are received. Although some nodes will want the highest accuracy possible, this speed can be beneficial in cases when the target can only send a small number of packets or needs a location estimate quickly.

7 LIMITATIONS AND FUTURE WORK

One limitation of *multipath triangulation* is that it relies on the existence of a propagation path going directly from transmitter to receiver. The evaluation demonstrates that it works well even in NLoS scenarios where the direct path is not the strongest signal, but in the case of complete blockage it will actually produce the

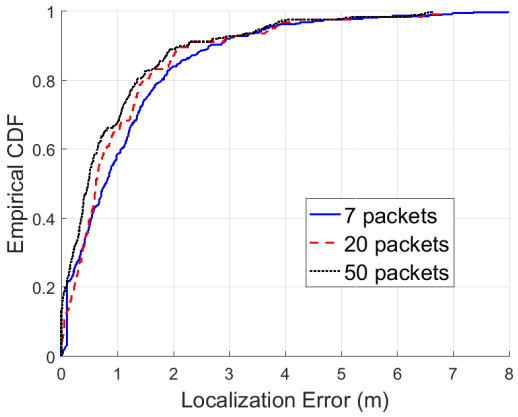

Figure 11: The cumulative distribution of localization error for 7, 20, and 50 packets shows that MonoLoco works well with small number of packets. All target locations in 4 deployments are aggregated in this graph.

wrong location estimate. Currently, all other decimeter-level WiFi localization systems also have this limitation, and localizing targets with no LoS path is still an open problem. A second limitation of *multipath triangulation* is that it requires a 3-element antenna array on both the transmitter and receiver, similar to Chronos [40]. As such, it cannot localize/orient small devices such as smart phones or smart watches that typically have only one antenna. However, many WiFi devices including laptops, APs, robots, and smart appliances do have 3-element antenna arrays, which are becoming more common with MIMO technology. MonoLoco can be used by a single autonomous robot to localize multiple APs, which could in-turn be used to localize single-antenna devices using protocols such as SpotFi [18]. Moreover, the presence of the 3-element array on the target is what enables orientation inference. Finally, *multipath triangulation* relies on first order reflections and assumes that the second order reflections are too weak to be resolved. In indoor environments, it is rare to receive a second order reflection, but if so, we can filter out these reflections in the post-processing step and use another pair of paths.

The main contributions of this paper are the new *multipath triangulation* techniques, and the 3D super-resolution algorithm to estimate the geometric features of multiple paths. These techniques are not limited to WiFi, and can be used in many ways besides single-device WiFi localization. MonoLoco is just a proof-of-concept for the wide range of applications where these techniques can produce substantial gains such as in indoor mapping, object imaging, or device-free localization. In future work, we plan to explore how MonoLoco could interact with WiCapture [19], which uses multipath reflections to provide accurate motion tracking. WiCapture can only get relative motion and not absolute position, so these two systems are complementary and could be combined. Additionally, the current version of MonoLoco uses a subspace super-resolution algorithm to resolve multipath features with a linear antenna array. However, the fundamental methods are independent of the multipath resolution technique and the antenna configuration. Therefore, we will explore how MonoLoco's performance could be improved by advances in multipath resolution such as the recent works in Maximal Likelihood Estimation techniques [46], larger antenna arrays, or circular antenna arrays.

8 CONCLUSION

This paper presents *multipath triangulation*, a new localization technique that leverages multipath reflections to estimate the location of a target and a reflector with respect to the receiver. We use *multipath triangulation* to develop MonoLoco, the first localization system that provides decimeter-level localization and orientation information without any information sharing or coordination across multiple nodes. A single WiFi node or access point can localize any other WiFi transmitter that it hears. The protocol is fully piggybacked on top of the WiFi protocol. We expect *multipath triangulation* and its use of multpath reflections for localization to lead a universal paradigm shift in IoT where the WiFi in every home and office can act as an efficient non-intrusive yet omnipresent sensing system which does not require new sensor hardware installation. We believe that *multipath triangulation* is more widely applicable to protocols other than WiFi and for problems other than target localization, including device tracking, indoor mapping, object imaging, and device free tracking, which are among our future works.

9 ACKNOWLEDGEMENTS

This work was funded in part by NSF grants 1305362 and 1739333. We thank our shepherd Souvic Sen and the anonymous reviewers for their valuable feedback. We also thank our colleagues at Stanford and Prof. Robert M. Weikle for technique advice on device calibration and Colin Rooney, the undergraduate assistant, for helping to build the platform.

REFERENCES

[1] F. Adib, C.-Y. Hsu, H. Mao, D. Katabi, and F. Durand. Capturing the human figure through a wall. *ACM Transactions on Graphics (TOG)*, 34(6):219, 2015.
[2] F. Adib, Z. Kabelac, and D. Katabi. Multi-person localization via rf body reflections. In *NSDI*, pages 279–292, 2015.
[3] F. Adib, Z. Kabelac, D. Katabi, and R. C. Miller. 3d tracking via body radio reflections. In *NSDI*, 2014.
[4] M. H. Afzal, V. Renaudin, and G. Lachapelle. Multi-magnetometer based perturbation mitigation for indoor orientation estimation. *Navigation*, 58(4):279–292, 2011.
[5] P. Bahl and V. N. Padmanabhan. Radar: An in-building rf-based user location and tracking system. In *INFOCOM 2000. Nineteenth Annual Joint Conference of the IEEE Computer and Communications Societies. Proceedings. IEEE*, volume 2, pages 775–784. Ieee, 2000.
[6] L. Chang, X. Chen, Y. Wang, D. Fang, J. Wang, T. Xing, and Z. Tang. Fitloc: Fine-grained and low-cost device-free localization for multiple targets over various areas. *IEEE/ACM Transactions on Networking (TON)*, 25(4):1994–2007, 2017.
[7] K. Chetty, G. E. Smith, and K. Woodbridge. Through-the-wall sensing of personnel using passive bistatic wifi radar at standoff distances. *IEEE Transactions on Geoscience and Remote Sensing*, 50(4):1218–1226, 2012.
[8] R. Elbakly and M. Youssef. A robust zero-calibration rf-based localization system for realistic environments. In *Sensing, Communication, and Networking (SECON), 2016 13th Annual IEEE International Conference on*, pages 1–9. IEEE, 2016.
[9] J. Gjengset, J. Xiong, G. McPhillips, and K. Jamieson. Phaser: Enabling phased array signal processing on commodity wifi access points. In *Proceedings of the 20th annual international conference on Mobile computing and networking*, pages 153–164. ACM, 2014.
[10] J. P. Godbaz, M. J. Cree, and A. A. Dorrington. Understanding and ameliorating non-linear phase and amplitude responses in amcw lidar. *Remote Sensing*, 4(1):21–42, 2011.
[11] D. Halperin, W. Hu, A. Sheth, and D. Wetherall. Predictable 802.11 packet delivery from wireless channel measurements. In *ACM SIGCOMM Computer Communication Review*, volume 40, pages 159–170. ACM, 2010.

[12] J. Haverinen and A. Kemppainen. Global indoor self-localization based on the ambient magnetic field. *Robotics and Autonomous Systems*, 57(10):1028–1035, 2009.

[13] F. Heide, M. B. Hullin, J. Gregson, and W. Heidrich. Low-budget transient imaging using photonic mixer devices. *ACM Transactions on Graphics (ToG)*, 32(4):45, 2013.

[14] A. R. Jimenez, F. Seco, C. Prieto, and J. Guevara. A comparison of pedestrian dead-reckoning algorithms using a low-cost mems imu. In *Intelligent Signal Processing, 2009. WISP 2009. IEEE International Symposium on*, pages 37–42. IEEE, 2009.

[15] A. Kalyanaraman, D. Hong, E. Soltanaghaei, and K. Whitehouse. Forma track: tracking people based on body shape. *Proceedings of the ACM on Interactive, Mobile, Wearable and Ubiquitous Technologies*, 1(3):61, 2017.

[16] A. Kim and M. Golnaraghi. A quaternion-based orientation estimation algorithm using an inertial measurement unit. In *Position Location and Navigation Symposium, 2004. PLANS 2004*, pages 268–272. IEEE, 2004.

[17] M. Kotaru. Supplementary material of wicapture. https://bitbucket.org/mkotaru/wicapturesourcecode.

[18] M. Kotaru, K. Joshi, D. Bharadia, and S. Katti. Spotfi: Decimeter level localization using wifi. In *ACM SIGCOMM Computer Communication Review*, volume 45, pages 269–282. ACM, 2015.

[19] M. Kotaru and S. Katti. Position tracking for virtual reality using commodity wifi. *arXiv preprint arXiv:1703.03468*, 2017.

[20] S. Krishnan, P. Sharma, Z. Guoping, and O. H. Woon. A uwb based localization system for indoor robot navigation. In *Ultra-Wideband, 2007. ICUWB 2007. IEEE International Conference on*, pages 77–82. IEEE, 2007.

[21] C. P. Kumar, R. Poovaiah, A. Sen, and P. Ganadas. Single access point based indoor localization technique for augmented reality gaming for children. In *Students' Technology Symposium (TechSym), 2014 IEEE*, pages 229–232. IEEE, 2014.

[22] S. Kumar, S. Gil, D. Katabi, and D. Rus. Accurate indoor localization with zero start-up cost. In *Proceedings of the 20th annual international conference on Mobile computing and networking*, pages 483–494. ACM, 2014.

[23] S. Lanzisera, D. Zats, and K. S. Pister. Radio frequency time-of-flight distance measurement for low-cost wireless sensor localization. *IEEE Sensors Journal*, 11(3):837–845, 2011.

[24] J.-Y. Lee and R. A. Scholtz. Ranging in a dense multipath environment using an uwb radio link. *IEEE Journal on Selected Areas in Communications*, 20(9):1677–1683, 2002.

[25] J. Lin, Y. Liu, M. B. Hullin, and Q. Dai. Fourier analysis on transient imaging with a multifrequency time-of-flight camera. In *Proceedings of the IEEE Conference on Computer Vision and Pattern Recognition*, pages 3230–3237, 2014.

[26] M. Mahfoudi, T. Turletti, T. Parmentelat, F. Ferrero, L. Lizzi, R. Staraj, and W. Dabbous. Orion: Orientation estimation using commodity wi-fi, 05 2017.

[27] A. T. Mariakakis, S. Sen, J. Lee, and K.-H. Kim. Sail: Single access point-based indoor localization. In *Proceedings of the 12th annual international conference on Mobile systems, applications, and services*, pages 315–328. ACM, 2014.

[28] P. Misra and P. Enge. Special issue on global positioning system. *Proceedings of the IEEE*, 87(1):3–15, 1999.

[29] J. C. Mosher and R. M. Leahy. Source localization using recursively applied and projected (rap) music. *IEEE Transactions on signal processing*, 47(2):332–340, 1999.

[30] L. M. Ni, Y. Liu, Y. C. Lau, and A. P. Patil. Landmarc: indoor location sensing using active rfid. *Wireless networks*, 10(6):701–710, 2004.

[31] V. N. Padmanabhan and L. Subramanian. Determining the geographic location of internet hosts. In *SIGMETRICS/Performance*, pages 324–325, 2001.

[32] N. B. Priyantha, A. Chakraborty, and H. Balakrishnan. The cricket location-support system. In *Proceedings of the 6th annual international conference on Mobile computing and networking*, pages 32–43. ACM, 2000.

[33] R. Schmidt. Multiple emitter location and signal parameter estimation. *IEEE transactions on antennas and propagation*, 34(3):276–280, 1986.

[34] S. Sen, B. Radunovic, R. R. Choudhury, and T. Minka. You are facing the mona lisa: spot localization using phy layer information. In *Proceedings of the 10th international conference on Mobile systems, applications, and services*, pages 183–196. ACM, 2012.

[35] A. Shahmansoori, G. E. Garcia, G. Destino, G. Seco-Granados, and H. Wymeersch. Position and orientation estimation through millimeter wave mimo in 5g systems. *arXiv preprint arXiv:1702.01605*, 2017.

[36] E. Soltanaghaei, A. Kalyanaraman, and K. Whitehouse. Peripheral wifi vision: Exploiting multipath reflections for more sensitive human sensing. In *Proceedings of the 4th International on Workshop on Physical Analytics*, pages 13–18. ACM, 2017.

[37] E. Soltanaghaei, A. Kalyanaraman, and K. Whitehouse. Poster: Occupancy state detection using wifi signals. In *Proceedings of the 15th Annual International Conference on Mobile Systems, Applications, and Services*, pages 161–161. ACM, 2017.

[38] C.-C. Tsai. A localization system of a mobile robot by fusing dead-reckoning and ultrasonic measurements. *IEEE Transactions on Instrumentation and Measurement*, 47(5):1399–1404, 1998.

[39] M. C. Vanderveen, C. B. Papadias, and A. Paulraj. Joint angle and delay estimation (jade) for multipath signals arriving at an antenna array. *IEEE Communications letters*, 1(1):12–14, 1997.

[40] D. Vasisht, S. Kumar, and D. Katabi. Decimeter-level localization with a single wifi access point. In *NSDI*, pages 165–178, 2016.

[41] C. Wang, Q. Yin, and H. Chen. Robust chinese remainder theorem ranging method based on dual-frequency measurements. *IEEE Transactions on Vehicular Technology*, 60(8):4094–4099, 2011.

[42] C. Wang, Q. Yin, and W. Wang. An efficient ranging method for wireless sensor networks. In *Acoustics Speech and Signal Processing (ICASSP), 2010 IEEE International Conference on*, pages 2846–2849. IEEE, 2010.

[43] J. Wang, H. Jiang, J. Xiong, K. Jamieson, X. Chen, D. Fang, and B. Xie. Lifs: low human-effort, device-free localization with fine-grained subcarrier information. In *Proceedings of the 22nd Annual International Conference on Mobile Computing and Networking*, pages 243–256. ACM, 2016.

[44] J. Wang, J. Xiong, H. Jiang, X. Chen, and D. Fang. D-watch: Embracing âĂIJbadâĂİ multipaths for device-free localization with cots rfid devices. *IEEE/ACM Transactions on Networking*, 25(6):3559–3572, 2017.

[45] J. Werb and C. Lanzl. Designing a positioning system for finding things and people indoors. *IEEE spectrum*, 35(9):71–78, 1998.

[46] Y. Xie, J. Xiong, M. Li, and K. Jamieson. xd-track: leveraging multi-dimensional information for passive wi-fi tracking. In *Proceedings of the 3rd Workshop on Hot Topics in Wireless*, pages 39–43. ACM, 2016.

[47] J. Xiong and K. Jamieson. Arraytrack: A fine-grained indoor location system. Usenix, 2013.

[48] J. Xiong, K. Jamieson, and K. Sundaresan. Synchronicity: pushing the envelope of fine-grained localization with distributed mimo. In *Proceedings of the 1st ACM workshop on Hot topics in wireless*, pages 43–48. ACM, 2014.

[49] J. Xiong, K. Sundaresan, and K. Jamieson. Tonetrack: Leveraging frequency-agile radios for time-based indoor wireless localization. In *Proceedings of the 21st Annual International Conference on Mobile Computing and Networking*, pages 537–549. ACM, 2015.

[50] J. Xu, M. Ma, and C. L. Law. Position estimation using uwb tdoa measurements. In *Ultra-wideband, the 2006 IEEE 2006 International Conference on*, pages 605–610. IEEE, 2006.

[51] M. Youssef, A. Youssef, C. Rieger, U. Shankar, and A. Agrawala. Pinpoint: An asynchronous time-based location determination system. In *Proceedings of the 4th international conference on Mobile systems, applications and services*, pages 165–176. ACM, 2006.

[52] G. V. Zàruba, M. Huber, F. Kamangar, and I. Chlamtac. Indoor location tracking using rssi readings from a single wi-fi access point. *Wireless networks*, 13(2):221–235, 2007.

[53] R. Zetik, S. Crabbe, J. Krajnak, P. Peyerl, J. Sachs, and R. Thomä. Detection and localization of persons behind obstacles using m-sequence through-the-wall radar. In *Sensors, and Command, Control, Communications, and Intelligence (C3I) Technologies for Homeland Security and Homeland Defense V*, volume 6201, page 62010I. International Society for Optics and Photonics, 2006.